

## Article

# Effects of Cold Plasma Treatment on Physical Modification and Endogenous Hormone Regulation in Enhancing Seed Germination and Radicle Growth of Mung Bean

Thi Quynh Xuan Le <sup>1,2</sup>, Linh Nhat Nguyen <sup>1</sup>, Thanh Tung Nguyen <sup>1</sup>, Eun Ha Choi <sup>3</sup>,  
Quang Liem Nguyen <sup>1</sup>, Nagendra Kumar Kaushik <sup>3,\*</sup> and Nguyen Thuan Dao <sup>1,2,\*</sup>

<sup>1</sup> Laboratory of Plasma Technology, Institute of Materials Science, Vietnam Academy of Science and Technology (VAST), 18 Hoang Quoc Viet Road, Cau Giay District, Hanoi 100000, Vietnam

<sup>2</sup> Graduate University of Science and Technology (GUST), VAST, Hanoi 100000, Vietnam

<sup>3</sup> Plasma Bioscience Research Center, Department of Electrical and Biological Physics, Kwangwoon University, Seoul 01897, Korea

\* Correspondence: kaushik.nagendra@kw.ac.kr (N.K.K.); thuandn@ims.vast.ac.vn (N.T.D.)

**Abstract:** This study investigated the effects of plasma duration and different reactive species ratios of cold atmospheric-pressure plasma treatment on both physical and endogenous hormone changes in enhancing the germination and growth of mung bean seeds. Seed germination and sprout stem length were significantly enhanced after plasma treatment. The germination rate increased eleven times after 12 h, while the radicles' length increased ~3 times after 96 h with optimal plasma treatment parameters. SEM images showed that the plasmas directly induced gradual changes in the seed coating, including deformed and shrunken epidermis, and cracks with sizes varying from 0.2 to 1.5  $\mu\text{m}$  after 4 min of plasma treatment. Water contact angle was reduced from 73° with untreated seed to almost 0° with 4 min treated seed. These effects could lead to better water absorption on the surface of treated seeds. We found that a plasma energy dosage of 0.08 Wh per seed and NO concentration between 20–95 ppm were the optimal enhancement conditions. We also showed that, for the first time, through delicate extraction, separation, and quantification processes, NO-induced upregulation of the natural growth hormone gibberellic acid could be the dominant phytochemistry pathway responsible for the enhancement effect.

**Keywords:** cold plasma; plasma in agriculture; seed germination enhancement; gibberellic acid; SEM; LC-MS



**Citation:** Le, T.Q.X.; Nguyen, L.N.; Nguyen, T.T.; Choi, E.H.; Nguyen, Q.L.; Kaushik, N.K.; Dao, N.T. Effects of Cold Plasma Treatment on Physical Modification and Endogenous Hormone Regulation in Enhancing Seed Germination and Radicle Growth of Mung Bean. *Appl. Sci.* **2022**, *12*, 10308. <https://doi.org/10.3390/app122010308>

Academic Editor: Emilio Martines

Received: 22 September 2022

Accepted: 11 October 2022

Published: 13 October 2022

**Publisher's Note:** MDPI stays neutral with regard to jurisdictional claims in published maps and institutional affiliations.



**Copyright:** © 2022 by the authors. Licensee MDPI, Basel, Switzerland. This article is an open access article distributed under the terms and conditions of the Creative Commons Attribution (CC BY) license (<https://creativecommons.org/licenses/by/4.0/>).

## 1. Introduction

Cold atmospheric-pressure plasma carries charged particles (i.e., electrons, ions), reactive oxygen species—ROS (such as hydroxyl radicals [OH], hydrogen peroxide [H<sub>2</sub>O<sub>2</sub>], singlet oxygen [O], ozone [O<sub>3</sub>], superoxide [O<sub>2</sub><sup>\*-</sup>]), reactive nitrogen species—RNS (such as nitrite [NO<sub>2</sub>], nitrate [NO<sub>3</sub>] and nitric oxide [NO]), and UV radiation, which can interact and have substantial effects on living organisms. In recent decades, cold plasma has been extensively studied and is widely applied in various fields, from skin cancer treatment [1], wound healing [2], surface and solution disinfection and decontamination [3], to sustainable agriculture [4,5]. In the latter application, cold plasma can be used to induce progressive changes in developmental and physiological processes in seeds, including improving seed resistance to stress and diseases [6], modifying and increasing the permeability of seed coats [7], reducing microbial population [8], and stimulating seed germination and seedling growth [9,10].

Mung bean (*Vigna radiata*) is a common economical crop in Southeast Asia. Diseases and abiotic stresses can lead to a considerable loss in nutritional quality and economic yield of mung beans, and are traditionally addressed through genetic engineering and the use of

growth-inducing chemicals, such as antibiotics [11]. However, not only can these chemicals be a danger to both humans and the environment, but excessive antibiotic treatments can also induce the development of antibiotic resistance, which makes them less effective. Therefore, a replacement of these chemicals with alternative treatments is beneficial.

Both the dormancy and germination of seeds are regulated by the balance of two endogenous natural plant hormones: abscisic acid (ABA) and gibberellic acid (GA<sub>3</sub>) [12]. ABA (C<sub>15</sub>H<sub>20</sub>O<sub>4</sub>) is known as the plant hormone responsible for the establishment of seed dormancy and prohibits germination, while higher levels of GA<sub>3</sub> (C<sub>19</sub>H<sub>22</sub>O<sub>6</sub>) are required to promote the release from dormancy, plant cell growth, and stem elongation. The activity of these hormones counteracts each other, and can depend on the concentration of reactive species such as hydrogen peroxide, nitrates, and nitric oxide [13]. However, their mechanisms are still far from being fully understood. Among reactive species generated by cold atmospheric-pressure gas-phase plasma, nitric oxide (NO) has been proven to induce the rapid decrease of ABA and promote GA<sub>3</sub> biosynthesis via competitive pathways, which in turn leads to breaking seed dormancy [14,15]. Recently, NO from cold plasma has been proposed to be able to regulate GA<sub>3</sub> in treated seeds [10,16], resulting in enhanced seed germination.

Although enhancing seed germination by cold plasma has been investigated in various plant species with different plasma configurations (dielectric barrier discharge—DBD, gliding arc, plasma jet) and a wide range of treatment protocols [10,17], the optimal parameters for enhancement effect have not been well established. Moreover, there is a lack of study on the phytochemistry pathway of how cold plasma treatment can enhance seed germination and growth of mung beans (*Vigna radiata*).

This work studied the effect of plasma duration and different reactive species ratios (RNS/ROS) of cold plasma treatment on both physical and endogenous hormone changes in enhancing seed germination and radicle growth of mung beans. While the physical changes on the seed's surface are dose-dependent, there are optimal "windows" for plasma energy dosage, and the NO concentration in the plasma induces the highest amount of up-regulated gibberellic acid, leading to better growth in the treated seeds. We believe that our findings can serve as a guide for plasma energy dosage, as well as the crucial NO concentration, to achieve the optimal effect of enhancing seed germination and plant growth, regarding any cold plasma setup.

## 2. Materials and Methods

### 2.1. Non-Thermal Atmospheric Pressure Plasma Jet Apparatus

Figure 1 shows the plasma jet emitter, which consisted of a stainless-steel needle inserted inside a 1.5-mm diameter quartz capillary tube, following a setup as reported in [18]. The metal needle, acting as one electrode, was covered with an insulating rubber, then attached to a quartz tube by adhesive epoxy. A ring-type copper electrode was made by wrapping copper tape outside the quartz tube at 1 cm below the tip of the needle electrode. The plasma downstream length (the length of the quartz tube below the ring electrode) was 5 cm. A high-frequency (40 KHz), high-voltage generator (5 kV) acted as a power supply to drive the plasma jet. The Argon gas was connected to a flow controller to maintain a constant gas flow rate at 400 sccm. The plasma power was ~1.2 W, as calculated using the area of the Lissajous diagram (Figure S1).

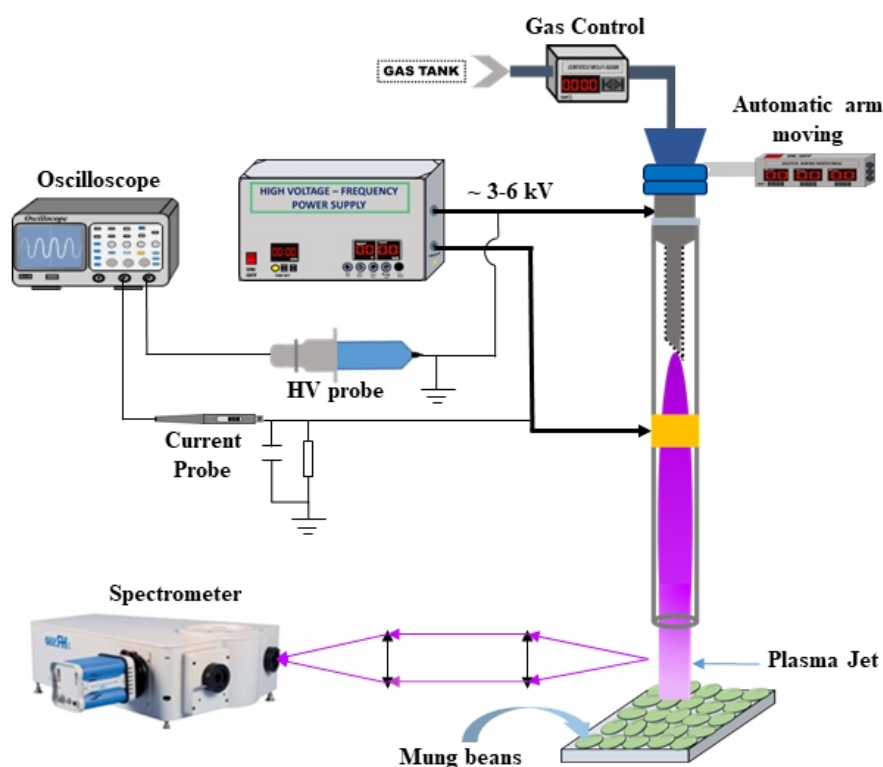


**Figure 1.** Experimental plasma jet system for treatment of mung bean seeds.

### 2.2. Electrical and Optical Spectroscopy Characterization of the Plasma Jet

A Tektronix P6015 voltage probe (1000:1) and a Tektronix current probe P6021A were connected to a Tektronix TBS1154 oscilloscope to measure the output voltage and current waveform of the plasma system.

The optical emission of the plasma jet discharge was collected 10 mm away from the nozzle and focused on the input of an IHR550 spectrometer. All spectra were scanned with an integration time of 0.1 s, excitation, and an emission slit width of 0.05 mm. Two gratings were used: a 150-grooves/mm grating with a resolution of 0.2 nm, and a 600 grooves/mm grating with a resolution of 0.05 nm. Three continuous scans were acquired and averaged to give an emission spectrum in all cases.

### 2.3. Enhancement of Seed Germination and Seedling Growth of Mung Bean

The seeds were pre-selected to ensure germination capability, and had similar sizes and shapes. A batch of 25 seeds was placed 10 mm below the plasma tip and exposed to an Ar-gas plasma jet for different treatment times: 1, 2, 4, 6, 8, 10, and 15 min. The plasma jet was continuously moved around the seeds by an automatic holder to guarantee equal plasma treatment for all seeds. These 25 seeds were then overspread, without touching each other, in a 90-mm diameter glass Petri dish, covered by a wet thin paper, and 5 mL of water was added to create the moisture conditions for germination. Meanwhile, the controlled seeds were also subjected to the same conditions as the treated seeds: Ar gas flow, but without plasma treatment. All samples were incubated in a humidity cabinet (Taisite, model: RGX400) with a set-up at room temperature  $\sim 28$  °C to ensure all seeds were grown under the same conditions. During germination and growth, 5 mL of distilled water was added every 12 h to each petri dish to maintain moisture conditions. Seed growth was observed, and the number of germinated seeds was recorded every 12 h. Each experiment contained 5 batches (a total of 125 seeds per experiment). The germination rate was defined as:

$$\text{Germination rate} = \frac{\text{total number of germinated seeds}}{\text{total number of seeds}} \times 100\% \quad (1)$$

#### 2.4. Scanning Electron Microscopy (SEM)

The surface morphology and integrity of the seeds were observed with SEM. Each sample was affixed to the surface of an aluminum stub with double-sided carbon tape. SEM was carried out on a Hitachi S-4800 field emission scanning electron microscope at 5 kV acceleration voltage.

#### 2.5. Extraction of Gibberellic Acid (GA<sub>3</sub>) Hormone

We followed a previous extraction protocol to extract Gibberellic acid (GA<sub>3</sub>) from untreated and plasma-treated seeds [19]:

1. 100 g of bean sprouts after 24 h of incubation (with and without plasma treatment) were dried at 65 °C for 12 h and ground into powder.
2. 5 g mung bean sprout powder and 50 mL MeOH were added to a conical beaker, shaken for 25 min, and then sonicated for 15 min.
3. After standing for 2.5 h at 4 °C, the supernatant was collected.
4. The remaining residue was further extracted with 25 mL MeOH, following the same steps as above.
5. The post-extraction solution was evaporated to dryness at 50 °C under a stream of nitrogen and then dissolved in 1 mL of double-distilled water.
6. The solution was filtered through a 0.45-mm Millipore filter before using for analysis.

#### 2.6. Separation and Confirmation of Gibberellic Acid (GA<sub>3</sub>) by LC-MS Analysis

To separate gibberellic acid (GA<sub>3</sub>) from the extracted solution, we used a Thermo Finnigan (Polaris Q) Ion Trap combined with a liquid chromatography-mass spectrometry (LC-MS) system. The analytical column was ZB-5 (30 m × 0.25 mm i.d., Zebron). The mobile phase was acetonitrile with 0.1% formic acid at a flow rate of 0.5 mL/min. An amount of 20 µL of each solution containing the extracted GA<sub>3</sub> was injected into the chromatograph and the absorption wavelength was detected at 195 nm.

To confirm whether the substance obtained after LC of the extraction solution was GA<sub>3</sub>, the ionization MS spectrum was obtained using electrospray ionization (ESI) in negative ion mode and at 550 °C, with N<sub>2</sub> gas to create a mist (nebulizer). The detection mode was multiple reaction monitoring (MRM) of selected ions in the first (Q1) and third (Q3) quadrupole filters.

### 3. Results and Discussion

#### 3.1. Effect of Cold Plasma Treatment on Physical Change of Seed's Surface

##### 3.1.1. Effect of Cold Plasma Treatment Time on Germination Rate and Root Length

Seed germination is a physiological process that begins with the seeds' water absorption (imbibition) and ends with the root emerging. To study the effect of the plasma energy dosage on seed germination, we applied different plasma treatment times (1, 2, 4, 6, 8, 10, and 15 min) and monitored both the germination rate and the lengths of the sprout roots after germination. Seed germination and root length were significantly enhanced after plasma treatment (Figure 2a). After 12 h of sowing on cotton under the same conditions, the germination rate, defined as the number of germinated seeds per the total number of seeds (Equation (1)), increased from 8% to 88% (11 times) between untreated and 15-min plasma-treated seeds (Figure 2b). After 24 h, all seeds were germinated, and the length of the root also significantly increased, from 70% in the range of 0.25–0.75 cm (group 2-red) for untreated seeds, to 70% in the range of 0.75–1.25 cm (group 3-green) for 4-min plasma-treated seeds, and up to 60% in the range of longer than 1.25 cm (group 4-blue) for 10-min plasma-treated seeds (Figure 2c). These results were obtained from five replications (a total of 125 seeds per a certain treatment time). Effect of plasma enhancement on the length of 24-h sprout root was saturated after 10 min of treatment, since 10-min and 15-min plasma treatments showed similar results. Our observation also agreed with a recent report [20], which indicated that short-time plasma treatment promoted seed germination and seedling growth, while long-time plasma treatment could have inhibitory effects. For the highest

germination rate after 12 h and the longest extrusion root after 24 h, a plasma treatment time of 10 min for 25 seeds with a plasma power of 1.2 W was optimal, which equaled a plasma energy dosage of 0.08 Wh per seed.

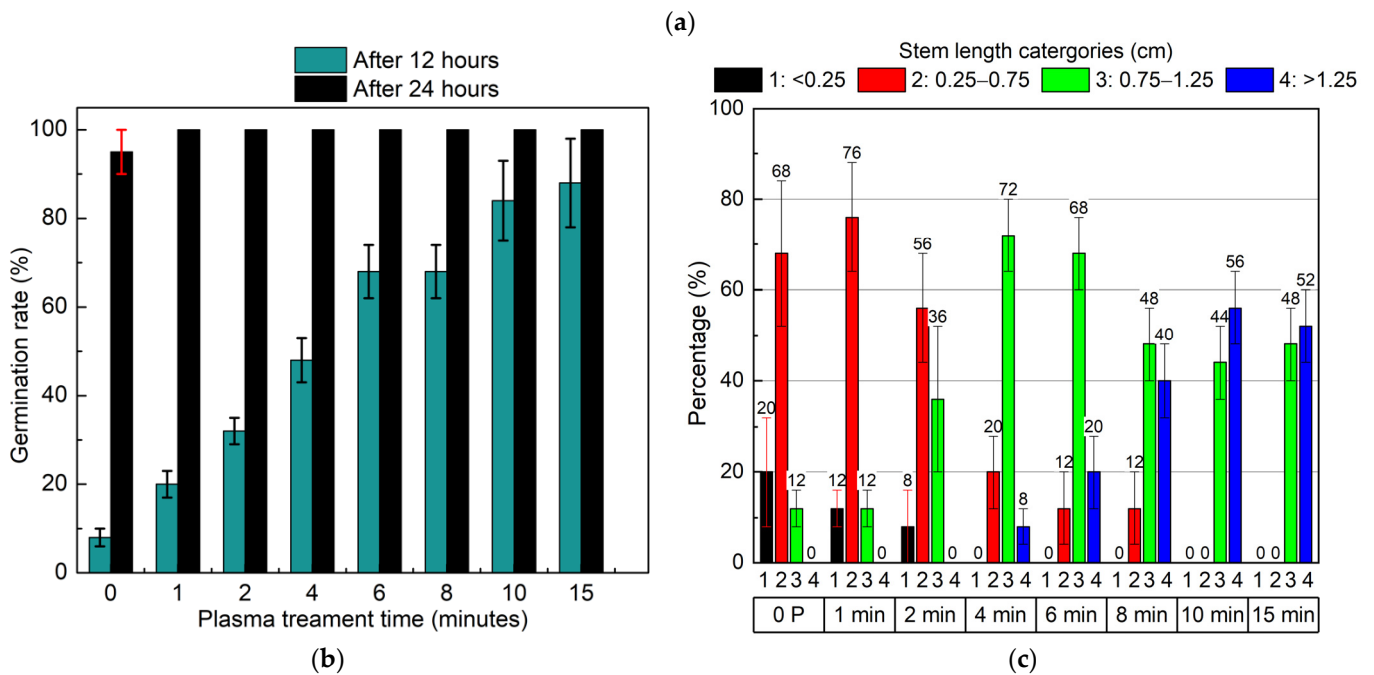
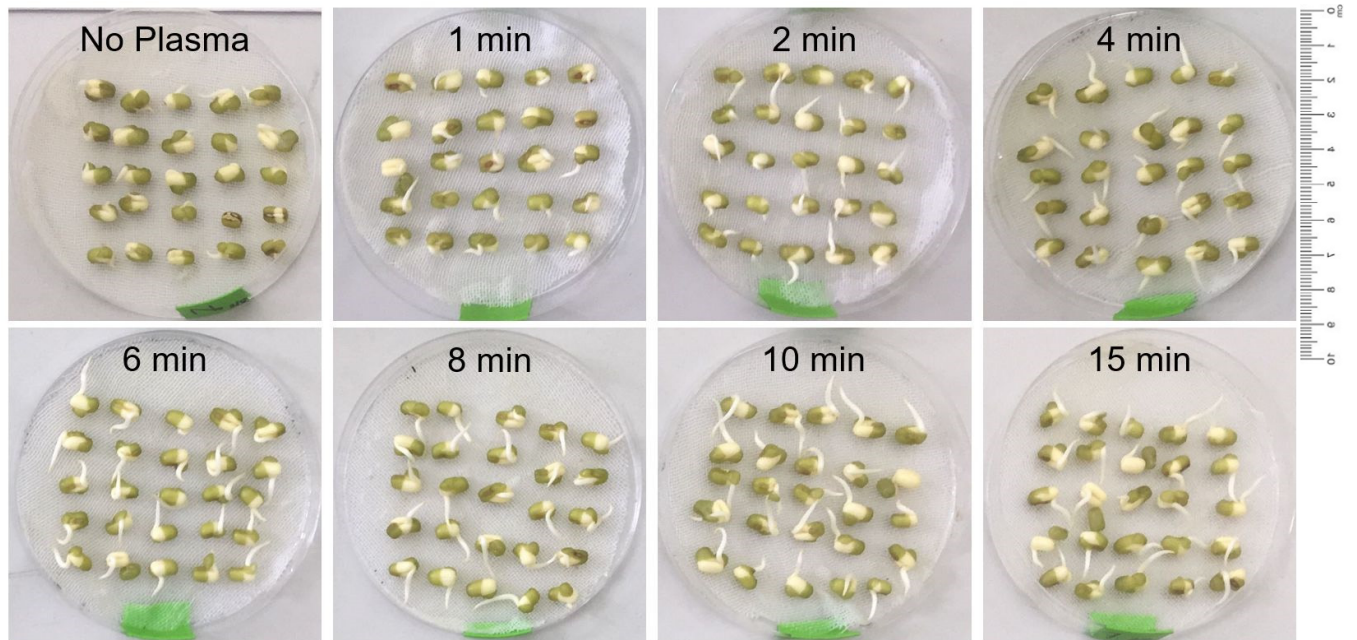


**Figure 2.** (a) Photo of batches of 25 bean sprout seeds with different plasma treatment time after 24 h of sowing on cotton on a 9-cm petri dish. The ruler on the right is 10-cm long. (b) Seed germination rate after 12 h and 24 h. (c) Effect of plasma treatment time on the roots at germination state. Plot of percentage of seeds divided into different categories of roots' length: (1-black): shorter than 0.25 cm; (2-red): 0.25–0.75 cm; (3-green): 0.75–1.25 cm; and (4-blue): longer than 1.25 cm. The error bar was calculated from five replications (total 125 seeds per a certain treatment time).

To understand the effect of enhancing germination and stem growth, we studied changes in the seed's surface morphology, wettability, as well as the regulation of gibberellic acid induced by plasma treatment.

### 3.1.2. Effect of Cold Plasma Treatment on Seeds' Surface Morphology

During early germination steps, the seed coating acts both as physical protection against the environment and as a constraint for root protrusion. Therefore, any structural modification of this coating could affect seed germination. To investigate the effect of cold plasma treatment on the seed's coating surface, scanning electron microscopy (SEM) was employed to characterize the seed's surface morphology.

SEM images suggest that the plasma directly induced changes in the seed coating (Figure 3). There are only slight deformations after 1-min plasma treatment and some wrinkles emerging on the seed surface after 2-min plasma treatment. However, the epidermis is deformed and shrunken in the seeds treated for 4 min. The surface topography of the seeds is comprised of crack features with sizes varying from 0.2 to 1.5  $\mu\text{m}$  after 4 min of plasma treatment. The degree of seed coat deformation and the size of the cracks are proportional to the plasma treatment time. We rule out the effect of UV radiation produced by the plasma jet in forming these cracks and deformation features, since exposing seeds to similar UV radiation by a UV lamp (peaked at 254 nm) at the same time as plasma treatment results in no change in the seed coating. Therefore, we relate these crack features to the interaction of the electrons and ions of the plasma with the seed coating. Our findings also agree with other reports, in which the cold plasma was observed to induce change in the outer coating of different seeds [7,21].

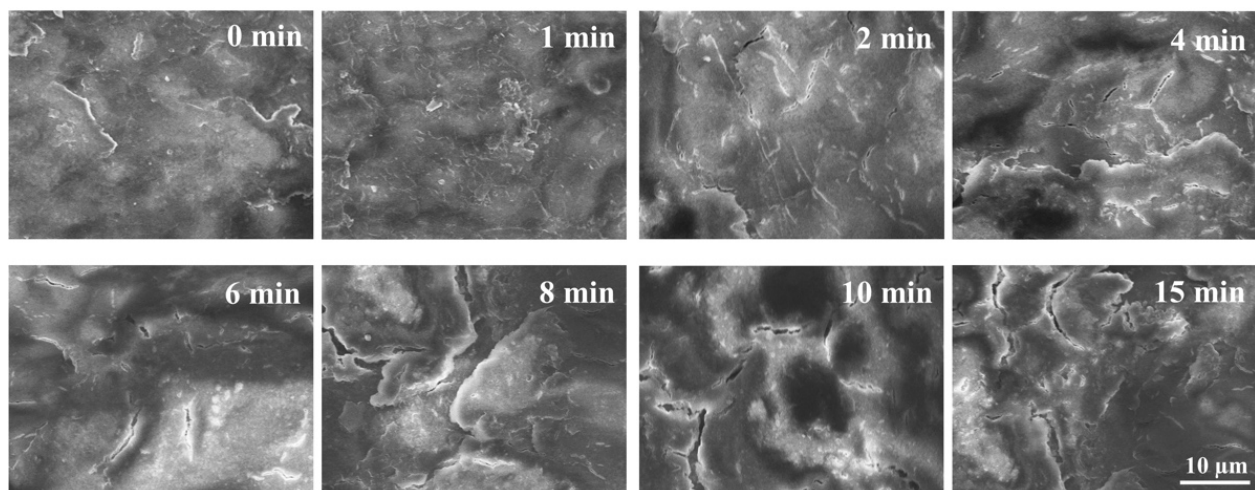


**Figure 3.** SEM images of the morphology of the seeds' surface without plasma treatment (0 min) and with 1, 2, 4, 6, 8, 10, and 15 min of plasma treatment.

### 3.1.3. Effect of Cold Plasma Treatment on the Wettability of Seeds

Figure 4 shows that plasma treatment caused a transition from partial to almost complete wetting between untreated and plasma-treated mung bean seeds. The water contact angle was determined in sessile drop mode with distilled water with a drop volume of 5  $\mu\text{L}$ . ImageJ software was used to measure static contact angles and the values of the three measurements were averaged. The water contact angle reduced from  $73^\circ$  with untreated seeds, to  $63^\circ$  with 1-min plasma treatment, to  $47^\circ$  with 2-min plasma treatment, and to almost  $0^\circ$  with seeds that were treated for longer than 4 min. This observation also agreed with other reports, in which plasma treatment led to a dramatic decrease in the apparent contact angle of different seeds [21,22]. More spreading and wetting and  $\mu\text{m}$ -sized cracks lead to better water absorption on the surface of treated seeds. Consequently, this effect could enhance the germination rate and promote the growth of the sprout stem. Moreover, the increase in hydrophilicity of the treated seeds might save a significant amount of water necessary for irrigation. A previous study performed on pea seeds demonstrated an acceleration in water uptake following treatment with cold plasmas [23].

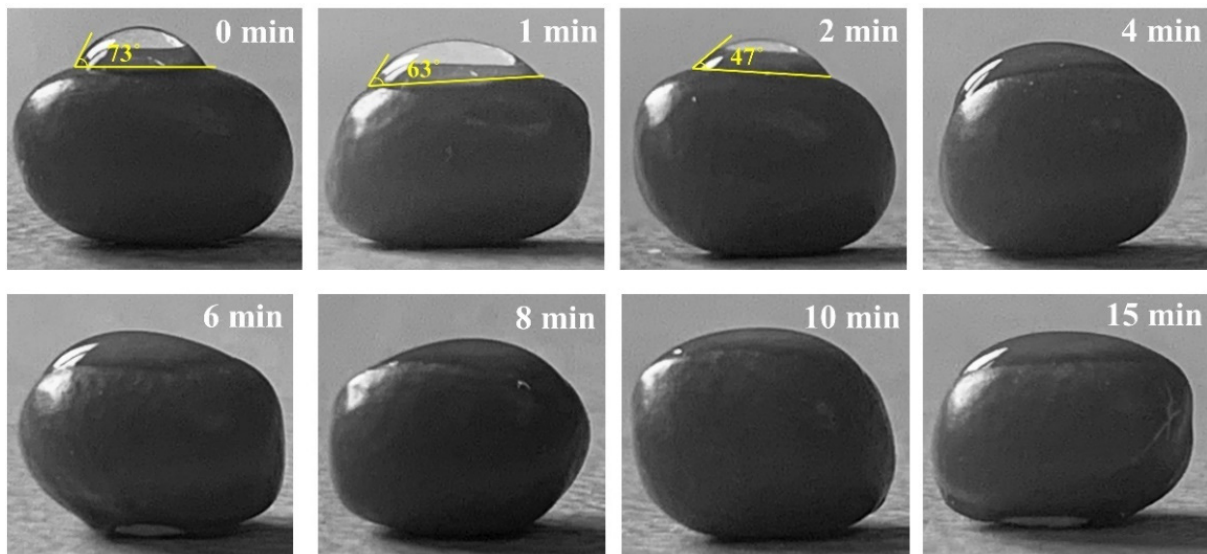


**Figure 4.** Water droplets deposited on mung bean seeds with untreated (0 min) and 1, 2, 4, 6, 8, 10, and 15 min of plasma treatment.

While the physical changes on the seed's surface were dose-dependent, and the change in the wettability of seeds was saturated after 4 min of plasma treatment, longer plasma treatment induced a higher germination rate and better development of the radices, and the enhancement effect only saturated after 10 min of plasma treatment. Therefore, not only physical changes induced by plasma treatment, but also the “chemical” changes in the endogenous hormone of the seeds, can even have a higher responsibility for this enhancement effect. The influence of cold plasma treatment on the genetics of seeds and other biological factors—such as the endogenous hormones that result in enhanced seed growth—remains unclear. Here, we varied the ratio of the plasma-generated reactive species while maintaining the maximum physical change condition (10 min plasma treatment time) to understand how they regulate  $GA_3$  and affect plant growth. We extracted, separated, and quantified  $GA_3$  from untreated and plasma-treated germinated seeds to study the effect of cold plasma treatment on this natural plant growth hormone.

### 3.2. Effect of Cold Plasma Treatment on Endogenous Hormone Regulation

#### 3.2.1. Regulation of Plasma-Generated Reactive Species (RNS/ROS)

We employed an advantage of the plasma jet configuration, which allows us to regulate the ratio of the plasma-generated reactive species (RNS/ROS) by simply adjusting the downstream length of the plasma jet [24]. We created five plasma jet tubes (1, 3, 5, 7, and 10 cm, hence named T1, T3, T5, T7, and T10, respectively) at different downstream lengths (the length of the quartz tube below the ring electrode), while maintaining a constant 1-cm upstream length (Figure 5a). Since the distance between the two electrodes was kept constant, the discharge pattern and discharge current were almost identical for different plasma tube lengths. The dissipated power of the plasma jets, estimated using the area of the Lissajous diagram, was calculated to be in the range of 1–1.4 W.

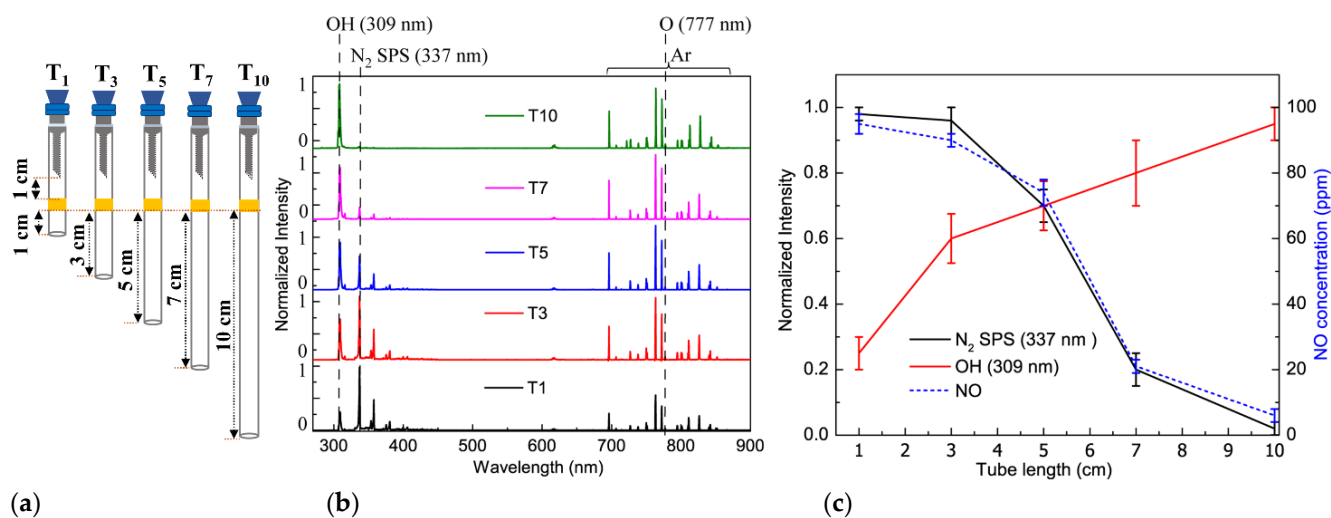


**Figure 5.** (a) Different downstream tube lengths. (b) Optical emission spectra in 270–900 nm range. (c) Dependence of optical emission intensities from N<sub>2</sub> SPS (337 nm), OH radical (309 nm), and NO concentration with different downstream tube lengths.

To examine the components emitted from the Ar plasma jets, we measured their optical emission spectra in a broad range region of 270–900 nm, as shown in Figure 5b. The emission peaks at 650–900 nm regions were due to the transition from 4p excited Ar levels (2p<sub>i</sub> in Paschen’s notation) to the 4s ground levels or metastable states (1s<sub>i</sub> in Paschen’s notation). Because the grating’s resolution in these measurements was 0.2 nm, the wavelength numbers were taken to the nearest integer. A weak emission peak at 777 nm was due to the atomic O. In the 300–400 nm region, several peaks that belonged to Nitrogen species (in particular, 337-nm peak from N<sub>2</sub> SPS—second positive system) and a 309-nm peak that belonged to OH radicals were also observed. While N<sub>2</sub> is abundant in ambient air, the water vapor from the air inside the capillary was excited into OH radical under the plasma discharge, which exhibited an emission at 309 nm. An electrochemical sensor PAC 800 from Dräger coupled with a nitrogen oxide (NO) gas detector (8326350) was used to measure the concentration of the gas-phase NO. The gas sensor was pre-calibrated to avoid interference from other compounds generated by the plasma gas. The density of NO rapidly increased over time and became stable after one minute. Figure 5c shows, as the downstream tube length increases, the emission intensity of N<sub>2</sub> SPS decreases (and the NO concentration also decreases accordingly), while the emission intensity of OH radical increases, indicating a higher RNS/ROS ratio is generated by the plasma jet with shorter downstream tube length.

### 3.2.2. Effect of Cold Plasma Treatment on Endogenous Hormone Regulation and Radicle Growth

To study how different RNS/ROS ratios in the plasma jet affected the regulation of the endogenous growth hormone GA<sub>3</sub>, seeds were treated by plasma jet with different tube lengths, and their radicle growth was monitored up to 96 h. The optimal plasma treatment time of 10 min obtained from the previous section was applied in all cases. We followed a previous extraction protocol to extract GA<sub>3</sub> from untreated and plasma-treated seeds [19] as described in the methods. Figure S2 shows liquid chromatograms of the extracted liquid vs. the calibration curve of the standard GA<sub>3</sub>. The retention time of GA<sub>3</sub> was from 7 to 8 min, peaking at 7.9. To confirm whether the substance obtained after LC from the extraction solution was GA<sub>3</sub>, we measured the MS spectrum of the extracted liquid from 7 to 8 min retention time. Figure 6a shows the MS spectrum of GA<sub>3</sub> separated from the extraction solution. In addition to a peak at 345.1 (*m/z*) corresponding to [M–H]<sup>–</sup> ion, we obtained a peak at 239.1 (*m/z*) corresponding to [M–H–COO–COO–H<sub>2</sub>O]<sup>–</sup> ion of

GA<sub>3</sub>. These peaks agreed with a previously published MS spectrum of GA<sub>3</sub> [25]; further confirming our successful extraction and separation of GA<sub>3</sub>.

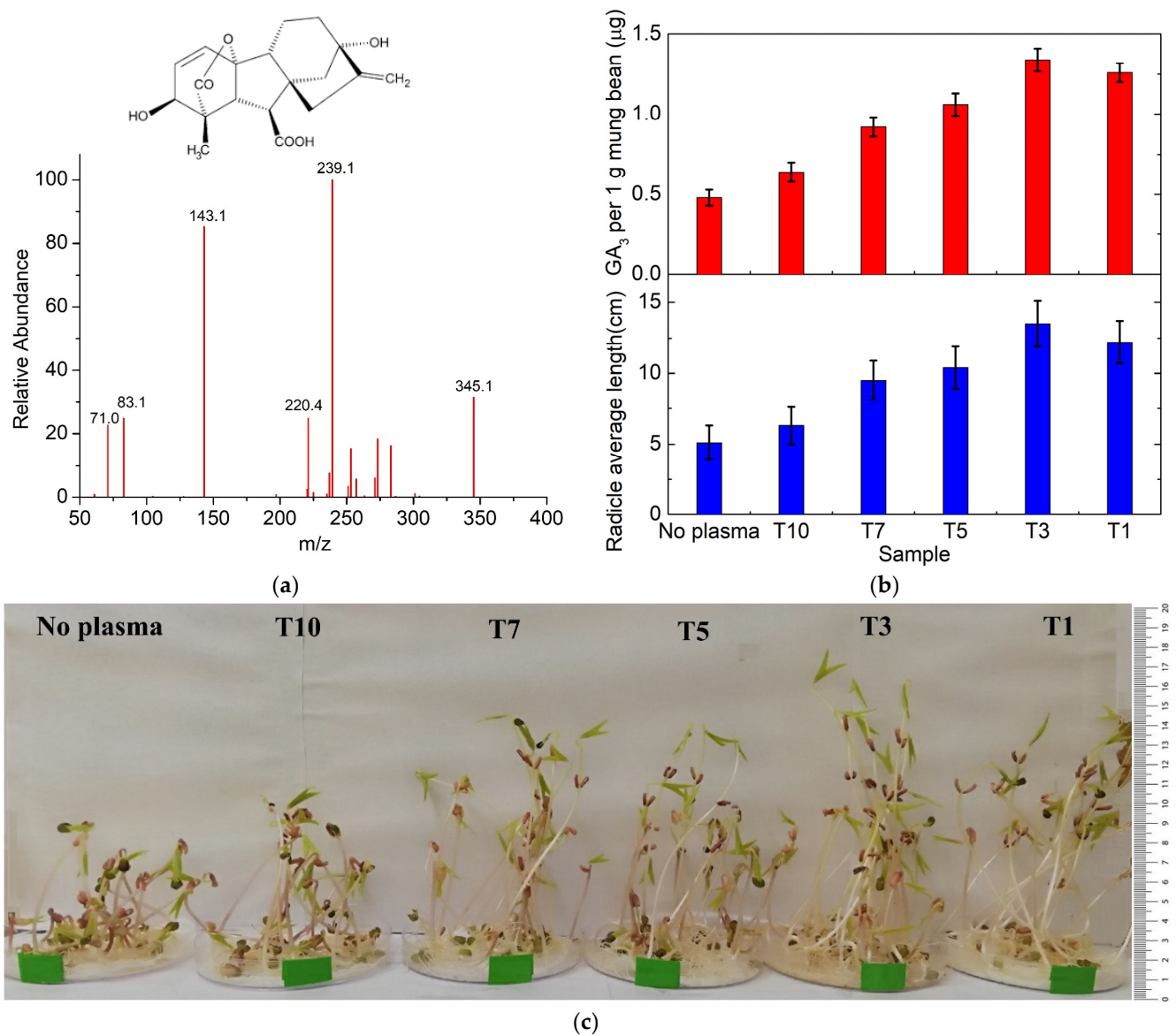


**Figure 6.** (a) Mass spectrum (MS) and the chemical structure (above) of GA<sub>3</sub> from the extracted solution. (b) The amount of GA<sub>3</sub> (red, above) extracted per 1 g mung bean; the average length of the radicles (blue, below), and (c) a photo of the radicles after 96 h under no plasma and plasma treatment with different downstream tube lengths. The ruler on the right is 20-cm long.

For quantitative analysis of GA<sub>3</sub>, a calibration curve was constructed with the standard GA<sub>3</sub> at seven different amounts (0.1; 0.5; 1; 2; 3; 5; 10) μg based on LC spectrum (Figure S3). The amount of gibberellic acid (GA<sub>3</sub>) in the extracted solution was determined based on the integrated area of the LC spectrum. Based on the quantitative calibration curve of GA<sub>3</sub>, through three average measurements, we determined the amount of GA<sub>3</sub> (μg) in 1 g bean sprout powder in each sample, as shown in Figure 6b (red, above). We observed that the shorter downstream tube length—hence the higher RNS/ROS ratio—led to upregulating GA<sub>3</sub> in the treated seeds. The amount of GA<sub>3</sub> reaches a maximum value of  $1.34 \pm 0.07$  μg per 1 g bean sprout powder (which is ~2.8 times more than untreated seeds) with the 3-cm plasma downstream tube length (T3). This result was the first direct measurement to show that cold plasma treatment can induce upregulation of the natural

endogenous hormone GA<sub>3</sub>, which leads to enhancing germination and radicle growth of treated seeds.

Interestingly, the plant growth of the radicles correspondingly followed the change in the regulated GA<sub>3</sub> (Figure 6b). The average length of the radicles also reached its maximum value of  $13.5 \pm 1.6$  cm (which is 2.7 times more than in the untreated seed) with T3 plasma jet. This result suggested that NO-induced upregulation of GA<sub>3</sub> by gas-phase cold plasma could be the dominant phytochemistry pathway responsible for enhancing the radicle growth of mung bean. Therefore, for the highest induced GA<sub>3</sub> concentration in seeds and the longest plant growth of the radicles, we recommend NO concentration between 20–95 ppm, which corresponds to the plasma downstream tube length from 7 cm (T7) to 1 cm (T1) (Figure 6c). We noted that the 1-cm plasma downstream tube length (T1) with too high RNS/ROS ratio resulted in the less effective enhancement of radicle growth, since high NO concentration can induce stress and interplay with the regulated GA<sub>3</sub> via plant signaling networks, and reduce GA<sub>3</sub> biosynthesis [26,27].

#### 4. Conclusions

We have demonstrated cold plasma treatment could be used as a quick, chemical-free, and effective method to enhance seed germination and seedling growth of mung beans. Both seed germination and radicles were significantly enhanced after plasma treatment. The germination rate increased eleven times after 12 h, while the radicles' length increased around three times after 96 h with optimal plasma treatment parameters. SEM images suggested that the plasmas induce gradual changes in the seed coating and wettability of the seeds. These effects could lead to better water absorption on the surface of treated seeds, and consequently, could enhance the germination rate and promote the growth of the sprout radicles. Through this study, we recommend a plasma energy dosage of 0.08 Wh per seed and NO concentration between 20–95 ppm as the crucial and optimal enhancement conditions. We also show that, for the first time, through delicate extraction, separation, and quantification processes, plasma treatment could induce up to three times higher regulation of natural plant growth hormone GA<sub>3</sub>, which could be mainly responsible for phytochemistry pathways of enhancing radicle growth. Finally, further studies are needed to fully understand the influence of cold plasma on the genetic and epigenetic changes of the treated seeds.

**Supplementary Materials:** The following supporting information can be downloaded at: <https://www.mdpi.com/article/10.3390/app122010308/s1>, Figure S1: Characteristics of the plasma jet: (A) voltage–current wavefunction and (B) Lissajous graph of the Ar plasma jet. The dissipated plasma power was estimated using a capacitance C means of 1 nF. Figure S2: (A) Liquid chromatograms of the extracted liquid (blue) vs. (B) the calibration curve of the standard GA<sub>3</sub> (Sigma—48880) (black). The retention time of GA<sub>3</sub> is from 7 to 8 min, peaking at 7.9. The amount of gibberellic acid (GA<sub>3</sub>) in extracted solution is determined based on the integrated area of the LC spectrum, with averaging of three measurements. Figure S3: Calibration curve derived from the integrated area between 7 to 8 min retention time in the LC spectrum vs. different amounts (0.1; 0.5; 1; 2; 3; 5; 10) µg of the standard GA<sub>3</sub>.

**Author Contributions:** Conceptualization, Q.L.N., N.K.K. and N.T.D.; methodology, L.N.N. and N.T.D.; software, T.Q.X.L., T.T.N. and N.T.D.; validation, T.Q.X.L. and N.T.D.; formal analysis, T.Q.X.L. and N.T.D.; investigation, T.Q.X.L., T.T.N. and N.T.D.; resources, T.Q.X.L. and N.T.D.; data curation, T.Q.X.L. and N.T.D.; writing—original draft preparation, T.Q.X.L. and N.T.D.; writing—review and editing, N.K.K. and N.T.D.; visualization, T.Q.X.L. and N.T.D.; supervision, E.H.C., Q.L.N., N.K.K. and N.T.D.; project administration, N.T.D.; funding acquisition, N.K.K., E.H.C., N.T.D. All authors have read and agreed to the published version of the manuscript.

**Funding:** This research was funded by IMS, VAST, grant number CS.14/20-21. This research is also supported by NRF Korea (2021R1A6A1A03038785, 2021R1F1A1055694).

**Institutional Review Board Statement:** Not applicable.

**Informed Consent Statement:** Not applicable.

**Data Availability Statement:** Not applicable.

**Acknowledgments:** We acknowledge Vee Vee Cheong and Derrick Jing Yang Tan from the School of Physical and Mathematical Sciences, Nanyang Technological University, Singapore for their help in LC-MS analysis and fruitful discussion. We thank Ta Ngoc Bach from IMS, VAST for his help in SEM measurement.

**Conflicts of Interest:** The authors declare no conflict of interest. The funders had no role in the design of the study; in the collection, analyses, or interpretation of data; in the writing of the manuscript; or in the decision to publish the results.

## References

1. Gay-Mimbrera, J.; García, M.C.; Isla-Tejera, B.; Rodero-Serrano, A.; García-Nieto, A.V.; Ruano, J. Clinical and biological principles of cold atmospheric plasma application in skin cancer. *Adv. Ther.* **2016**, *33*, 894–909. [[CrossRef](#)] [[PubMed](#)]
2. Bekeschus, S.; Schmidt, A.; Weltmann, K.-D.; von Woedtke, T. The plasma jet kINPen-A powerful tool for wound healing. *Clin. Plasma Med.* **2016**, *4*, 19–28. [[CrossRef](#)]
3. Scholtz, V.; Pazlarova, J.; Souskova, H.; Khun, J.; Julak, J. Nonthermal plasma—A tool for decontamination and disinfection. *Biotechnol. Adv.* **2015**, *33*, 1108–1119. [[CrossRef](#)]
4. Zhang, X.; Liu, D.; Zhou, R.; Song, Y.; Sun, Y.; Zhang, Q.; Niu, J.; Fan, H.; Yang, S.-Z. Atmospheric cold plasma jet for plant disease treatment. *Appl. Phys. Lett.* **2014**, *104*, 043702. [[CrossRef](#)]
5. Bourke, P.; Ziuzina, D.; Boehm, D.; Cullen, P.J.; Keener, K. The potential of cold plasma for safe and sustainable food production. *Trends Biotechnol.* **2018**, *36*, 615–626. [[CrossRef](#)] [[PubMed](#)]
6. Ling, L.; Jiangang, L.; Minchong, S.; Chunlei, Z.; Yuanhua, D. Cold plasma treatment enhances oilseed rape seed germination under drought stress. *Sci. Rep.* **2015**, *5*, 13033. [[CrossRef](#)]
7. Bafoil, M.; Jemmat, A.; Martinez, Y.; Merbahi, N.; Eichwald, O.; Dunand, C.; Yousfi, M. Effects of low temperature plasmas and plasma activated waters on Arabidopsis thaliana germination and growth. *PLoS ONE* **2018**, *13*, e0195512. [[CrossRef](#)]
8. Darmanin, M.; Fröhling, A.; Bußler, S.; Durek, J.; Neugart, S.; Schreiner, M.; Blundell, R.; Gatt, R.; Schlüter, O.; Valdramidis, V.P. Aqueous and gaseous plasma applications for the treatment of mung bean seeds. *Sci. Rep.* **2021**, *11*, 19681. [[CrossRef](#)]
9. Volin, J.C.; Denes, F.S.; Young, R.A.; Park, S.M.T. Modification of seed germination performance through cold plasma chemistry technology. *Crop Sci.* **2000**, *40*, 1706–1718. [[CrossRef](#)]
10. Waskow, A.; Howling, A.; Furno, I. Mechanisms of plasma-seed treatments as a potential seed processing technology. *Front. Phys.* **2021**, *9*, 174. [[CrossRef](#)]
11. Cao, J.; Wang, Y.; Wang, G.; Ren, P.; Wu, Y.; He, Q. Effects of typical antimicrobials on growth performance, morphology and antimicrobial residues of mung bean sprouts. *Antibiotics* **2022**, *807*, 807. [[CrossRef](#)] [[PubMed](#)]
12. Tuan, P.A.; Kumar, R.; Rehal, P.K.; Toora, P.K.; Ayele, B.T. Molecular mechanisms underlying Abscisic acid/Gibberellin balance in the control of seed dormancy and germination in cereals. *Front. Plant Sci.* **2018**, *9*, 668. [[CrossRef](#)] [[PubMed](#)]
13. Adhikari, B.; Adhikari, M.; Park, G. The effects of plasma on plant growth, development, and sustainability. *Appl. Sci.* **2020**, *10*, 6045. [[CrossRef](#)]
14. Liu, Y.; Shi, L.; Ye, N.; Liu, R.; Jia, W.; Zhang, J. Nitric oxide-induced rapid decrease of abscisic acid concentration is required in breaking seed dormancy in Arabidopsis. *New Phytol* **2009**, *183*, 1030–1042. [[CrossRef](#)] [[PubMed](#)]
15. Ji, S.H.; Kim, T.; Pannong, K.; Hong, Y.J.; Pengkit, A.; Park, D.H.; Kang, M.H.; Lee, S.H.; Im, J.S.; Kim, J.S.; et al. Assessment of the effects of nitrogen plasma and plasma-generated nitric oxide on early development of coriandrum sativum. *Plasma Process. Polym.* **2015**, *12*, 1164–1173. [[CrossRef](#)]
16. Zhang, S.; Rousseau, A.; Dufour, T. Dufour, Promoting lentil germination and stem growth by plasma activated tap water, demineralized water and liquid fertilizer. *RSC Adv.* **2017**, *7*, 31244–31251. [[CrossRef](#)]
17. Attri, P.; Koga, K.; Okumura, T.; Shiratani, M. Impact of atmospheric pressure plasma treated seeds on germination, morphology, gene expression and biochemical responses. *Jpn. J. Appl. Phys.* **2021**, *60*, 040502. [[CrossRef](#)]
18. Xuan, L.T.Q.; Nguyen, L.N.; Dao, N.T. Synthesis of stabilizer-free, homogeneous gold nanoparticles by cold atmospheric-pressure plasma jet and their optical sensing property. *Nanotechnology* **2021**, *33*, 105603. [[CrossRef](#)]
19. Sun, Y.-N.; Qin, S.-Y.; Lv, Y.-K.; Li, S.-Z.; Wei, C. Simultaneous determination of five phytohormones in mungbean sprouts of China by micellar electrokinetic chromatography. *J. Chromatogr. Sci.* **2013**, *52*, 725–729. [[CrossRef](#)]
20. Cui, D.; Hu, X.; Yin, Y.; Zhu, Y.; Zhuang, J.; Wang, X.; Ma, R.; Jiao, Z. Quality enhancement and microbial reduction of mung bean (*Vigna radiata*) sprouts by non-thermal plasma pretreatment of seeds. *Plasma Sci. Technol.* **2022**, *24*, 045504. [[CrossRef](#)]
21. Zhou, R.; Zhou, R.; Zhang, X.; Zhuang, J.; Yang, S.; Bazaka, K.; Ostrikov, K. Effects of atmospheric-pressure N<sub>2</sub>, He, Air, and O<sub>2</sub> microplasmas on mung bean seed germination and seedling growth. *Sci. Rep.* **2016**, *6*, 32603. [[CrossRef](#)]
22. Bormashenko, E.; Gryniov, R.; Bormashenko, Y.; Drori, E. Cold radiofrequency plasma treatment modifies wettability and germination speed of plant seeds. *Sci. Rep.* **2012**, *2*, 741. [[CrossRef](#)] [[PubMed](#)]
23. Stolárik, T.; Henselová, M.; Martinka, M.; Novák, O.; Zahoranová, A.; Černák, M. Effect of low-temperature plasma on the structure of seeds, growth and metabolism of endogenous phytohormones in pea (*Pisum sativum* L.). *Plasma Chem. Plasma Process.* **2015**, *35*, 659–676. [[CrossRef](#)]

24. Lamichhane, P.; Acharya, T.R.; Kaushik, N.; Nguyen, L.N.; Lim, J.S.; Hessel, V.; Kaushik, N.K.; Choi, E.H. Non-thermal argon plasma jets of various lengths for selective reactive oxygen and nitrogen species production. *J. Environ. Chem. Eng.* **2022**, *10*, 107782. [[CrossRef](#)]
25. Xie, W.; Han, C.; Zheng, Z.; Chen, X.; Qian, Y.; Ding, H.; Shi, L.; Lv, C. Determination of Gibberellin A3 residue in fruit samples by liquid chromatography–tandem mass spectrometry. *Food Chem.* **2011**, *127*, 890–892. [[CrossRef](#)] [[PubMed](#)]
26. Shah, T.; Wahid, S.; Ilyas, M.; Hasanuzzaman, M. Nitric oxide and phytohormones cross-talk during abiotic stresses responses in plants. In *Reactive Oxygen, Nitrogen and Sulfur Species in Plants*; John Wiley & Sons Ltd.: Hoboken, NJ, USA, 2019; pp. 533–554.
27. Wu, A.P.; Gong, L.; Chen, X.; Wang, J.X. Interactions between nitric oxide, gibberellic acid, and phosphorus regulate primary root growth in *Arabidopsis*. *Biol. Plant* **2014**, *58*, 335–340. [[CrossRef](#)]